International Journal of Nanomedicine

Dovepress
open access to scientific and medical research

Open Access Full Text Article

ORIGINAL RESEARCH

Investigation Of Vitamin B_{12}-Modified Amphiphilic Sodium Alginate Derivatives For Enhancing The Oral Delivery Efficacy Of Peptide Drugs

This article was published in the following Dove Press journal:
International Journal of Nanomedicine

Lingli Long,[1,2,*] Minghua Lai,[3,*] Xuhong Mao,[4] Jiahao Luo,[3] Xin Yuan,[2] Li-Ming Zhang,[4] Zunfu Ke,[5] Liqun Yang,[3] David YB Deng[1,2]

[1]Department of Research Center of Translational Medicine, The First Affiliated Hospital, Sun Yat-sen University, Guangzhou 510080, People's Republic of China; [2]Department of Scientific Research Center and Orthopedic, The Seventh Affiliated Hospital, Sun Yat-sen University, Shenzhen 518107, People's Republic of China; [3]Department of Polymer and Material Science, School of Chemistry, Key Laboratory for Polymeric Composite and Functional Materials of Ministry of Education, Guangdong Provincial Key Laboratory for High Performance Polymer-based Composites, Sun Yat-sen University, Guangzhou 510275, People's Republic of China; [4]Faculty of Materials Science and Engineering, Sun Yat-sen University, Guangzhou 510275, People's Republic of China; [5]Department of Pathology, The First Affiliated Hospital, Sun Yat-sen University, Guangzhou 510080, People's Republic of China

*These authors contributed equally to this work

Correspondence: David YB Deng
Department of Research Center of Translational Medicine, The First Affiliated Hospital, Sun Yat-sen University, Guangzhou 510080, People's Republic of China
Email dengyub@mail.sysu.edu.cn

Liqun Yang
Department of Polymer and Material Science, School of Chemistry, Key Laboratory for Polymeric Composite and Functional Materials of Ministry of Education, Guangdong Provincial Key Laboratory for High Performance Polymer-based Composites, Sun Yat-sen University, Guangzhou 510275, People's Republic of China
Email yanglq@mail.sysu.edu.cn

Purpose: Peptide drugs have been used in therapy various diseases. However, the poor bioavailability of peptide drugs for oral administration has limited their clinical applications, on account of the acidic environment and digestive enzymes inside the human gastrointestinal tract. To enhance stability in the human gastrointestinal tract, bioavailability, and targeted drug delivery of peptide drugs through oral administration, a vitamin B_{12}-modified amphiphilic sodium alginate derivative (CSAD-VB_{12}) was synthesized.

Materials and methods: A vitamin B_{12}-modified amphiphilic sodium alginate derivative (CSAD-VB_{12}) was synthesized via the N,N'-dicyclohexylcarbodiimide active method at room temperature, and then characterized using FTIR and ^{1}H NMR spectroscopy. Insulin was used as a model peptide drug and the insulin-loaded CSAD-VB_{12} (CSAD-VB_{12}/insulin) nanoparticles with negative zeta potentials were prepared in PBS (pH=7.4). Scanning electron microscopy was used to observe CSAD-VB_{12}/insulin as spherical nanoparticles. The CSAD-VB_{12} derivatives and CSAD-VB_{12}/insulin nanoparticles displayed nontoxicity towards the human colon adenocarcinoma (Caco-2) cells by CCK-8 test. Caco-2 cell model was used to measure the apparent permeability (Papp) of insulin, CSAD/insulin and CSAD-VB_{12}/insulin. Furthermore, confocal was used to confirm the endocytosis of intestinal enterocytes. Type 1 diabetes mice were used to evaluate the intestinal absorption and retention effect of test nanoparticles.

Results: They were observed as spherical nanoparticles in the size of 30–50 nm. The CSAD-VB_{12} derivatives and CSAD-VB_{12}/insulin nanoparticles displayed nontoxicity towards the human colon adenocarcinoma (Caco-2) cells. Comparing with insulin and the CSAD/insulin nanoparticles, the CSAD-VB_{12}/insulin nanoparticles exhibited higher permeation ability through intestinal enterocytes in the Caco-2 cell model. Oral administration of the CSAD-VB_{12}/insulin nanoparticles to Type 1 diabetic mice yields higher intestinal retention effect, targeted absorption, and outstanding efficacy.

Conclusion: CSAD-VB_{12} derivatives enhance the small intestinal absorption efficacy and retention of peptide by oral administration, which indicated that it could be a promising candidate for oral peptide delivery in the prospective clinical application.

Keywords: nanoparticle, insulin, human colon adenocarcinoma cell, small intestinal absorption efficacy

Introduction

Peptide drugs show low absorption efficacy via oral administration because of their low stabilities in the acidic environment of the stomach, degradation of digestive enzymes (such as pepsin and trypsin) inside the human gastrointestinal tract (GIT), poor diffusion across the small intestinal mucus layer, and low absorption by

epithelium cells.[1–3] As a promising new drug delivery technology, the utilization of polymeric nanoparticles for oral delivery of drugs can improve drug absorption efficacy by passing through intestinal barriers and thus increase bioavailability through possible transcellular and paracellular pathways.[1,3,4]

The transcellular pathway via the vitamin B_{12} (VB_{12}) absorption pathway has been identified as one of the most promising options for the oral delivery of peptides encapsulated in nanoparticles.[2,5] Since the net charge on peptides usually changes from positive to negative as the pH is increased from below to above their isoelectric point, peptides tend to be attracted to networks consisting of anionic polymers (such as alginate, carrageenan, or pectin) at low pH values below their isoelectric point.[1] Previous works reported that peptide drugs were protected from low gastric pH value and enzymatic hydrolysis by being encapsulated in anionic polymeric nanoparticles (such as insulin-encapsulated lactic-co-glycolic acid nanoparticles).[1,6]

Alginate is a linear anionic polysaccharide consisting of 1,4-β-D-mannuronic acid and α-L-guluronic acid (G) residues.[7] As a natural polysaccharide, sodium alginate has been found increasing biomedical applications because of advantages such as excellent cytocompatibility, biodegradability, non-toxicity, non-immunogenicity, and chelating ability.[8] In addition, alginate has been proved as an effective inhibitor of P-glycoprotein efflux pump that limits oral bioavailability through the transcellular pathway.[9] Since the electrostatic attraction between alginate and peptides (or proteins) occurs below around pH 3.5,[1] alginate hydrogel beads, alginate nanoparticles, and microparticles crosslinked by calcium ions have been prepared for protection of peptide and protein drugs from low gastric pH value and enzymatic hydrolysis.[10–12] To improve their stabilities and absorption efficacies in the small intestinal, alginate nanoparticles and microparticles were commonly coated with chitosan shell.[12–14]

Amphiphilic polysaccharide derivatives are potential drug carriers of peptides (or proteins) because they could assemble to form nanoparticles through intermolecular interactions.[15] Therefore, in this work, in order to prepare the nanoparticles for enhancing oral delivery efficacy of peptide drugs, the amphiphilic sodium alginate derivatives (CSAD) were synthesized based on our previous work.[7] As a small intestinal targeting factor, VB_{12} was conjugated with the CSAD derivative to yield the amphiphilic sodium alginate derivatives containing vitamin B_{12} (CSAD-VB_{12}, Scheme 1A) using the mild N,N'-carbonyldiimidazole

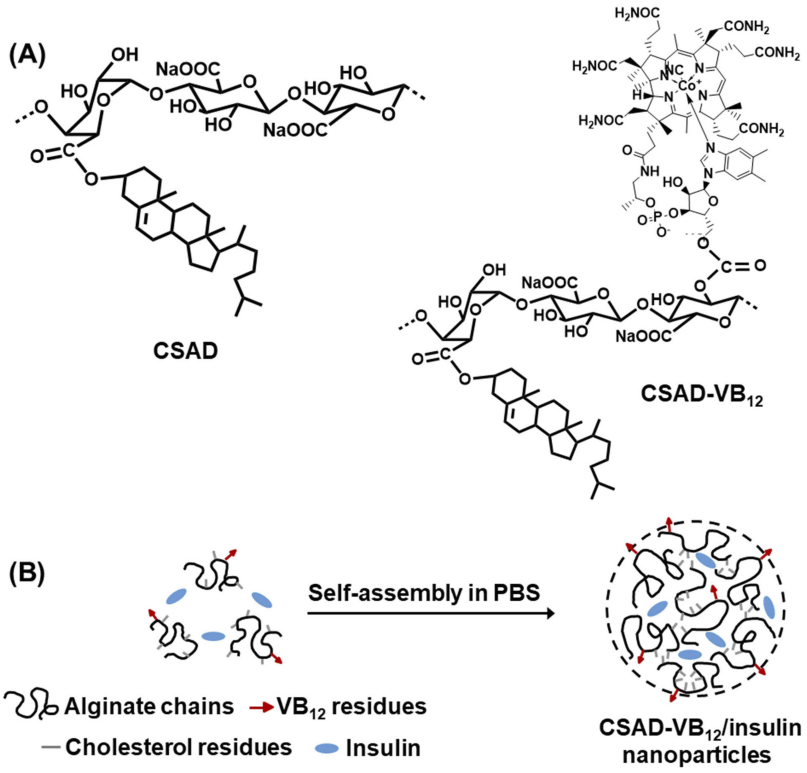

Scheme 1 (**A**) Chemical structures of the CSAD derivative and CSAD-VB_{12} derivative and (**B**) proposed self-assembly mechanism of CSAD-VB_{12}/insulin nanoparticles.

(CDI) activation method.[16,17] Actually, numerous peptide drugs have been successfully conjugated with VB_{12} to enhance their oral absorption[18,19] as VB_{12} can bind to salivary haptocorring in stomach at the first[20] and then associated with intrinsic factor (IF) in intestine. IF-receptor was located on the intestine epithelium, by which VB_{12} can be efficiently and fastly transcytosed through epithelium. From 1970s, VB_{12} has been used to increase pharmaceutical delivery because of this IF/IF-receptor dietary uptake pathway.[21]

Structures of CSAD and CSAD-VB_{12} were characterized by FTIR and ^{1}H NMR spectroscopy. Insulin was used as a model peptide drug and the insulin-loaded CSAD-VB_{12} (CSAD-VB_{12}/insulin) nanoparticles were prepared in PBS (pH=7.4) (Scheme 1B). Monolayers of human colon adenocarcinoma (Caco-2) cells are widely used as an effective model to study passive drug absorption across the intestinal epithelium in vivo human absorption. The Caco-2 cells are derived from a human colorectal adenocarcinoma cell line and retain many features of small intestinal cells.[2,22,23] The permeation of the CSAD-VB_{12}/insulin nanoparticles through intestinal enterocytes was thus evaluated in vitro using the Caco-2 cell monolayer model.

Materials And Methods

Materials

Alginate acid, cholesterol, N,N′-dicyclohexylcarbodiimide (DCC), and 4-(N,N′-dimethylamino) pyridine (DMAP) were purchased from Acros Organics (Janssens Pharmaceuticalaan, Belgium). Vitamin B_{12} was purchased from Sigma (St Louis, USA). N,N′-carbonyldiimidazole (CDI) and dimethyl sulfoxide (DMSO) were acquired from Aladdin Reagent Company (Shanghai, China), and DMSO was dried by soaking in molecular sieves and calcium hydride for a week before use. Cell counting kit-8 (CCK-8) was purchased from Dojindo Molecular Technologies Inc. (Kumamoto, Japan). The FITC-labelled insulin (FITC-insulin) was purchased from a biotechnological company (ZKCYBIO, Beijing, China). All other reagents obtained were of analytical grade and used without further purification.

Synthesis And Characterization Of The CSAD-VB_{12} Derivative

The CSAD derivative was synthesized based on our previous work.[7,8] Briefly, alginate acid (1.0 g, 5.68 mmol of uronic acid unit) was dissolved in 35 mL of water-free DMSO at room temperature overnight. Solutions of cholesterol (0.40 g, 1.10 mmol) in 2 mL chloroform and DCC (0.24 g, 1.16 mmol) and DMAP (0.14 g, 1.13 mmol) in 15 mL of DMSO were then added. The reaction was allowed to proceed for 24 hrs at room temperature, followed by purification with ethanol. The product was dried in vacuum at 40ºC for 24 hrs to obtain the CSAD derivative.

Following the CDI activation method used in previous work,[16,17] the CSAD-VB_{12} derivative was synthesized (Scheme 2). The CSAD derivative (0.10 g, 0.440 mmol uronic acid units) was dissolved in 20 mL of water-free DMSO. VB_{12} (0.30 g, 0.022 mmol) was dissolved in 10 mL of water-free DMSO, activated by adding CDI (0.04 g, 0.250 mmol), and then stirred for 1 hr in a nitrogen atmosphere at room temperature. After the reactive VB_{12} solution was added to the solution of the CSAD derivative, the reaction was allowed to proceed for 24 hrs in a dark, nitrogen atmosphere at room temperature. The product of CSAD-VB_{12} derivative in the reaction mixture was precipitated by adding 400 mL of acetone and centrifugated (3500 rpm, 20 mins). The obtained precipitation was dissolved in the distilled water and neutralized by adding $NaHCO_3$ solution (4%, w/v). The solution was dialyzed against the distilled water for 3 days and lyophilized to obtain the solid CSAD-VB_{12} derivative.

FTIR measurement was performed with an FTIR Analyzer (Nicolet/Nexus 670, Thermo Nicolet Corporation WI, USA) from 4000 to 400 cm^{-1} at a resolution of 4 cm^{-1} for 32 scans using the KBr method. ^{1}H NMR analysis was carried out on a Bruker AVANCE AV 400HD Superconducting Fourier NMR Spectrometer (Bruker BioSpin, Switzerland) at 25°C using D_2O as a solvent. The signal at δ 4.67 ppm for HDO was used as the internal standard.

The degree of substitution (DS) of the cholesterol residues of the CSAD derivative, defined as the number of cholesterol residues per uronic acid monomer unit of sodium alginate, was estimated using the ^{1}H NMR integral method. The DS value of the VB_{12} residues of the CSAD-VB_{12} derivative was determined using UV-vis spectroscopy. Briefly, the absorbance spectra of VB_{12} and the CSAD-VB_{12} derivative were obtained on a UV–vis spectrophotometry (UV-3150, Shimadzu, Japan). The VB_{12} standard solutions were prepared with DMSO at concentrations ranging from 6.0 to 50 μl/mL. Based on the absorbance of the peak at about 360 nm, the working curve was obtained (R^2=0.999). The CSAD-VB_{12} solution was prepared in DMSO, and the concentration of the VB_{12} residues was estimated according to the working curve,

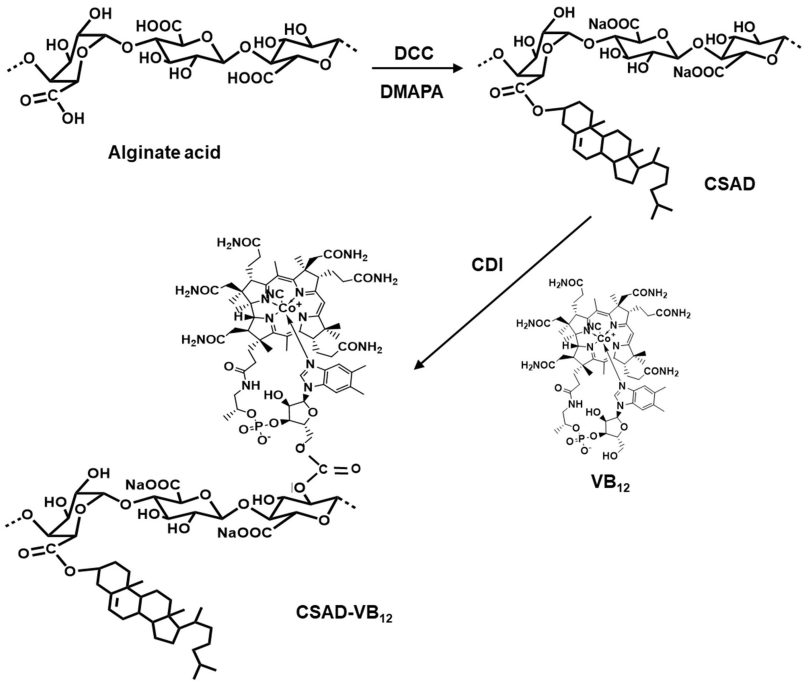

Scheme 2 Synthesis of the CSAD and CSAD-VB_{12} derivatives.

and then the DS value of the VB_{12} residues of the CSAD-VB_{12} derivative was calculated.

Preparation And Physicochemical Property Of CSAD-VB_{12}/Insulin Nanoparticles

The CSAD-VB_{12} derivative (30 mg) was dissolved in 9.0 mL of PBS (pH=7.4) and stirred at room temperature for 24 hrs. Three microliters of PBS (pH=7.4) containing insulin (10 mg/mL) was then added to the CSAD-VB_{12} solution, and the resulting mixture was stirred at room temperature for 24 hrs. The mixture was then centrifugated (25,000 rpm, 30 mins). A working curve for the insulin concentration in PBS (pH 7.4) and a wavelength of 276 nm was used to determine the amount of insulin in the supernatant (R^2 = 0.997), which was analyzed by UV–vis spectroscopy. The amount of insulin encapsulated in the nanoparticles was calculated based on the reduction in the insulin concentration. The insulin encapsulating capacity was then calculated using Equation (1).

$$\text{Encapsulating capacity}\,(\%) = [(W_0 - W_s)/W] \times 100 \quad (1)$$

where W_0 is the total weight of insulin used, W_s is the weight of un-encapsulated insulin in the supernatant, and W is the weight of the CSAD-VB_{12} derivative. Consequently, the insulin encapsulating capacity of the CSAD-VB_{12} nanoparticles was determined to be 35%. The CSAD/insulin nanoparticles were prepared using the same method.

The obtained hydrogel precipitation following centrifugation was dissolved in 10 mL of PBS (pH 7.4) to yield the solution of CSAD-VB_{12}/insulin nanoparticles. The zeta potential and hydrodynamic diameter were measured using ZetaPALS (Brookhaven Instruments Corporation, Holtsville, NY, USA) at 25°C. Each measurement was performed in triplicate. The CSAD-VB_{12}/insulin solution was dropped onto a tinfoil, and then dried at room temperature. Morphology was observed on an S-4800 scanning electron microscope (HI-9056-0003, Hitachi, Japan) after the sample was sputter-coated with gold in an E-1045 ion sputter (Hitachi, Japan).

In Vitro Insulin Release Profiles Of The CSAD-VB_{12}/Insulin Nanoparticles

Release studies were conducted at 37±0.5°C and a rotation speed of 100 r/min inside a YS–200 B water bath constant temperature oscillator (Yao Instrument Co, Ltd, Shanghai, China). According to the method used in the literature,[24,25] the insulin release profiles of the CSAD-VB_{12}/insulin nanoparticles were evaluated in the simulated stomach fluid containing pepsin (pH=1.2), the simulated duodenum fluid containing pepsin and trypsin (pH=4.5), and the simulated small intestinal fluid containing trypsin (pH=6.8).

Briefly, ten milliliters of PBS buffer (pH=7.4) containing CSAD-VB_{12}/insulin nanoparticles and CSAD/insulin nanoparticles were enclosed in a dialysis bag (molecular weight cutoff 8000 Da), which was immersed in 150 mL of simulated stomach fluid, duodenum fluid, and small intestinal fluid in consequence for 3, 1, and 3 hrs, respectively. At predetermined time intervals, 1.0 mL of buffer solution outside the dialysis bag was removed and replaced with 1.0 mL of fresh buffer solution. The amount of released insulin was analyzed by UV-vis spectrophotometry at 276 nm as mentioned above. The cumulative release percentage of insulin was calculated according to Equation (2).

$$\text{Cumulative release percentage} = (W_{R-Ins}/W_{Ins}) \times 100 \quad (2)$$

where $W_{R\text{-}Ins}$ is the weight of released insulin and W_{Ins} is the weight of insulin loaded in the CSAD-VB_{12}/insulin nanoparticles. All experiments were conducted in triplicate.

Cell Culture

Caco-2 cells were obtained from the American type culture collection (ATCC, Manassas, VA, USA). Cells were cultured in DMEM containing 10% fetal bovine serum (Invitrogen Corporation, Carlsbad, CA, USA), 100 units/mL penicillin, and 100 μg/mL streptomycin (medium A) at 37°C in a 5% CO_2 atmosphere. Caco-2 cells were differentiated into polarized epithelial monolayers by culturing on polypropylene membrane inserts of 35-mm Transwell plates (Corning Costar, Cambridge, MA) for 21 days in completed DMEM.

Cytotoxicity Assay

Cytotoxicity of the CSAD and CSAD-VB_{12} derivatives, and the CSAD/Insulin and CSAD-VB_{12}/Insulin nanoparticles in Caco-2 cells were assessed by cell counting kit-8 (CCK-8; Dojindo Molecular 21 Technologies Inc., Kumamoto, Japan). Briefly, Caco-2 cells were plated in 96-well plate (approximately 1×10^5 cells/well respectively), and were incubated for 24 hrs at 37°C. After replacement with fresh medium, the CSAD and CSAD-VB_{12} derivatives as well as the CSAD/Insulin and CSAD-VB_{12}/Insulin nanoparticles with different CSAD and CSAD-VB_{12} concentrations were added to each well, respectively, for another 48 hrs. Cells were then incubated for an additional 2 hrs with CCK-8 reagent (100 μL/mL medium) and assessed at 450 nm of microplate reader (Thermo, 5 Varioskan Flash). Each experiment was reproduced in six different wells, and repeated three times. Absorbance was recorded and the relative cell viability was calculated. Normally, Caco-2 cells without any treatment were used as the control. Cell viability (%) was calculated in accordance with Equation (3).

$$\text{Cell viability}\,(\%) = (A_{450-E}/A_{450-C}) \times 100 \quad (3)$$

where $A_{450\text{-}E}$ and $A_{450\text{-}C}$ are the absorbance values of the experimental groups and the control group, respectively. All experiments were conducted in triplicate.

Endocytosis Of Caco-2 Cells Toward The CSAD-VB_{12}/FITC-Insulin Nanoparticles Confocal Laser Scanning Microscopy

Confocal laser scanning microscopy was used to investigate the endocytosis of Caco-2 cells toward CSAD-VB_{12}/insulin nanoparticles. Since the intrinsic fluorescence intensity of insulin was too weak to be visible in confocal laser scanning microscopic images, the FITC-insulin was used to prepare the CSAD-VB_{12}/FITC-insulin nanoparticles (containing 200 μg/mL of FITC-insulin). Caco-2 cells were seeded in 35-mm petri dishes (Corning, BP94S-01, USA.) with 14-mm microwell (MatTek, No. P35G-1.5-14-C), which were then installed in a chamber of confocal microscopy supplied by 5% CO_2 at 37°C for alive cells. The movement of Caco-2 cells with CSAD-VB_{12}/FITC-insulin nanoparticles was observed on a confocal microscopy (Zeiss, LSM880, Germany) in time series of 2 hrs.

Permeability Of Caco-2 Cell Monolayers For The CSAD-VB_{12}/Insulin Nanoparticles

Caco-2 cells were seeded onto polycarbonate filter inserts in 12-well Transwell dishes (Corning Costar Co., Cambridge, MA) at a density of 2×10^5 cells/cm^2 in DMEM. Caco-2 cells were maintained at 37°C in a humidified atmosphere containing 5% CO_2 for 21 days. Monolayers with a transendothelial electrical resistance value above 300 Ω cm^2 were used in this study. On the day of the transport experiments, the culture medium was replaced with Hank's balanced salt solution (HBSS). Before the assay, Caco-2 cell monolayers were rinsed twice and incubated with the DMEM medium for 1 hr. After removing the medium, the solution of insulin, the CSAD/Insulin, and CSAD-VB_{12}/Insulin nanoparticles were, respectively, added to the apical side of the transwell inserts, and 1.5 mL DMEM medium was added to the basolateral side of the transwell inserts. The cells were incubated for 60 mins at 37°C.

After the transportation of insulin, CSAD/Insulin, and CSAD-VB_{12}/Insulin nanoparticles through Caco-2 cell monolayers, the concentration of insulin in basolateral wells was assessed by the microplate. The apparent permeability (Papp) was calculated according to Equation (4).[26] All experiments were conducted in triplicate.

$$Papp = (dQ/dt) \times 1/(C_0 \times A) \quad (4)$$

where Papp is apparent permeability coefficient (cm/s), C_0 is initial concentration of the substances in the apical chamber (mol/mL), and A is the surface area of the membrane (cm^2).

Type 1 Diabetic Mice Model

The animal experiments of this study were carried out in full compliance with the Guide for the Care and Use of Laboratory Animals. All animal experiments were performed according to the protocol approved by the Institutional Animal Care and Use Committee of Sun Yat-sen University. The female and male KM mice (about 20–23 g, 8 weeks) were purchased from the Animal Experimental Center of Sun Yat-sen University. Type 1 diabetic mice were induced by intraperitoneal injection of streptozotocin (STZ, 70 mg/kg), dissolved in citric acid buffer (PH=4.4) after 12 hrs fasting and free water supply.[27]

Keeping water and food enough after injection, consumption of water and food were monitored daily. Fasting blood glucose level was recorded by an Accu-Chek glucose meter (Roche Diagnostics GmbH., Mannheim, Germany) every three days, after seven days; T1D diabetes was defined by fasting blood glucose more than 300 mg/dl.

Measurement Of Blood Glucose Levels

Mice were fasted for 12 hrs before measuring blood glucose levels. Then, the mice were divided into 4 groups with 3 mice in each group and treated with the following formulations, respectively: intragastric gavage of the CSAD/insulin, CSAD-VB_{12}/insulin (at the insulin dose of 50 IU/kg), saline (control group), and injections of solutions of insulin (50 IU/kg). Blood samples were collected from the caudal vein and the blood glucose level was measured immediately at time points of 0, 2, 4, 6, 8, 10, 12 hrs.

FITC-Insulin, CSAD/FITC-Insulin, CSAD-VB_{12}/FITC-Insulin Absorption In The Mice Ileum

TID mice were anesthetized by an intraperitoneal injection of 40 mg/kg sodium pentobarbital before a midline incision was made in the abdomen. FITC-Insulin, CSAD/FITC-insulin, CSAD-VB_{12}/FITC-insulin were injected to the ileum at an insulin dose of 50 IU/kg and two ends of the ileal segment were tied to form a 10-cm sac into which 1 mL of pH 7.4 PBS was syringed. Next, the mucus in the apical side of intestinal epithelium was embedded in O.C.T. Ten-mm-thick frozen sections were prepared using a cryomicrotome (CM1950, Lecia, Germany). Sections were labeled with DAPI, and then were observed by fluorescence microscope (Axio Scope.A1, Zeiss, Germany). The average fluorescent intensity (AFI) was quantified using an imaging software (Image ProPlus 6.0).

The Degradation Of FITC-Insulin, CSAD/FITC-Insulin, CSAD- VB_{12}/FITC-Insulin In Vivo

TID mice were anesthetized by an intraperitoneal injection of 40 mg/kg sodium pentobarbital, and then intragastric administration of FITC-Insulin, CSAD/FITC-insulin, CSAD- VB_{12}/FITC-insulin, respectively, was carried out. After 1 hr, the degradation of FITC-Insulin, CSAD/FITC-insulin, CSAD- VB_{12}/FITC-insulin in GI of T1D mice were observed by an in vivo animal imaging system (Carestream In Vivo Imaging System FXPRO, Woodbridge). Next, the mice ileum was isolated surgically. The degradation of FITC-Insulin, CSAD/FITC-insulin, CSAD- VB_{12}/FITC-insulin were observed by the same in vivo animal imaging system (Carestream In Vivo Imaging System FXPRO, Woodbridge). The average fluorescent intensity (AFI) was quantified using an imaging software (Image ProPlus 6.0).

Statistical Analysis

Data were presented as mean ± SD of experiments, and were analyzed by the computer program SPSS 19.0 (SPSS Inc., Chicago, IL, USA) by means of an unpaired two-tailed Student's t test. Results were considered statistically significant at a P value of <0.05.

Results

Synthesis And Structural Characterization Of The CSAD-VB_{12} Derivative

To improve insulin absorption efficacy through oral administration, CSAD and CSAD-VB_{12} derivatives were synthesized in sequence (Scheme 2). The CSAD derivative was firstly synthesized using DCC and DMAP as coupling reagents at room temperature.

The FTIR spectra of the CSAD derivative were shown in Figure 1. When compared with the FTIR spectrum of sodium alginate (Figure 1B), the following new peaks appeared in the FTIR spectrum of the CSAD derivative (Figure 1A): 1733 cm^{-1} (vibration of –C=O of carboxylic ester group, –COOR), 1600 and 1414 cm^{-1} (asymmetric symmetric and stretching vibrations of –C=O of sodium carboxylate group, –COONa), 1093 and 1033 cm^{-1} (vibration of –C–O–C– of glucosidic bond). The result indicated that the cholesterol residues were conjugated with the sodium alginate chains through the ester bond.

In the ^{1}H NMR spectrum of sodium alginate (Figure 2A), the multiple resonance peaks in the range of 3.0–5.5 ppm were assigned to the protons of uronic acid monomer unit of sodium alginate.[7] In contrast, new multiple peaks appeared in the range of 1.0–2.0 ppm in the ^{1}H NMR spectrum of CSAD (Figure 2B), which were assigned to the protons of the cholesterol residues,[7] indicating that the cholesterol residues were conjugated with the sodium alginate chains.[7] The DS value of the cholesterol residues of the CSAD derivative was determined to be 8% by integrating signals from the protons corresponding to the cholesterol residues (1.0–2.0 ppm) and the protons of sodium alginate (3.0–5.5 ppm).

VB_{12} was then activated by CDI and conjugated with the DA-Chit derivative at room temperature to yield the CSAD-VB_{12} derivative (Scheme 2). In the ^{1}H NMR spectrum of the CSAD-VB_{12} derivative (Figure 2C), the proton signals of sodium alginate (3.0–5.5 ppm) and cholesterol residues (1.0–2.0 ppm) were also observed. The ^{1}H NMR spectrum of the VB_{12} material was shown in Figure 2D. In contrast, the characteristic resonance peaks of VB_{12} protons were observed in the ^{1}H NMR spectrum of the VB_{12}-DA-Chit derivative (peaks labeled with the red stars), which were absent in the ^{1}H NMR spectrum of the CSAD derivative (Figure 2B). These results evidenced that both cholesterol residues and VB_{12} residues were conjugated with the sodium alginate chains. The DS value of the VB_{12} residues was determined to be 1.4 w/w % (or 0.2 mol% relative to the number of uronic acid monomer units) using UV-vis spectroscopy (Figure 3), which is closed to the VB_{12} content of VB_{12}-modified dextran-g-polyethyleneoxide cetyl ether that could enhance oral drug delivery efficacy.[28]

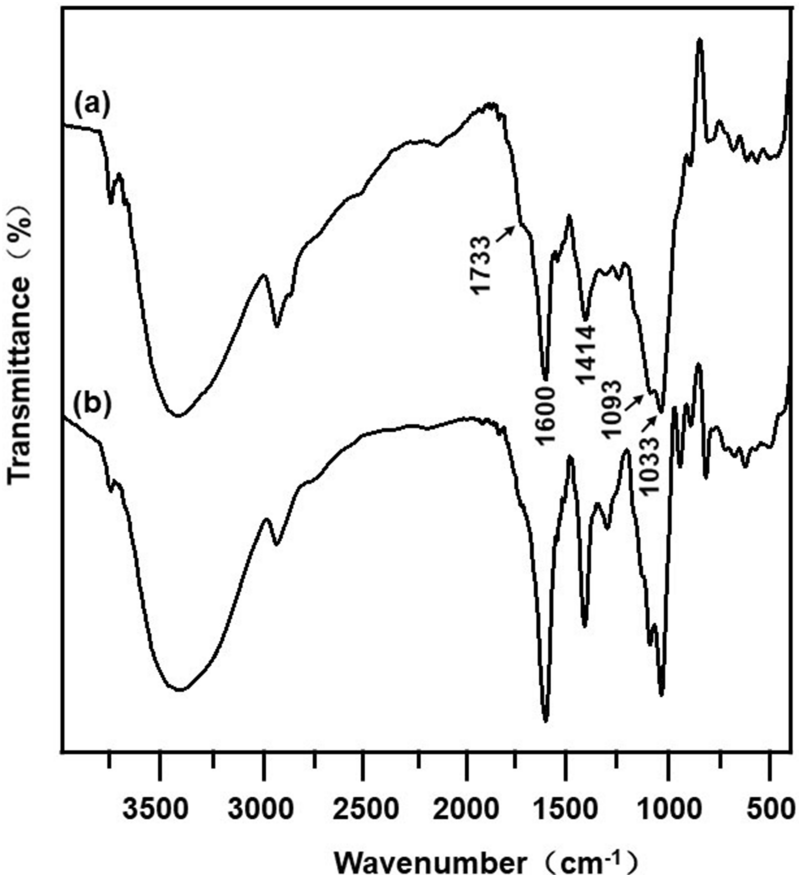

Figure 1 FTIR spectra of (**A**) the CSAD derivative and (**B**) sodium alginate.

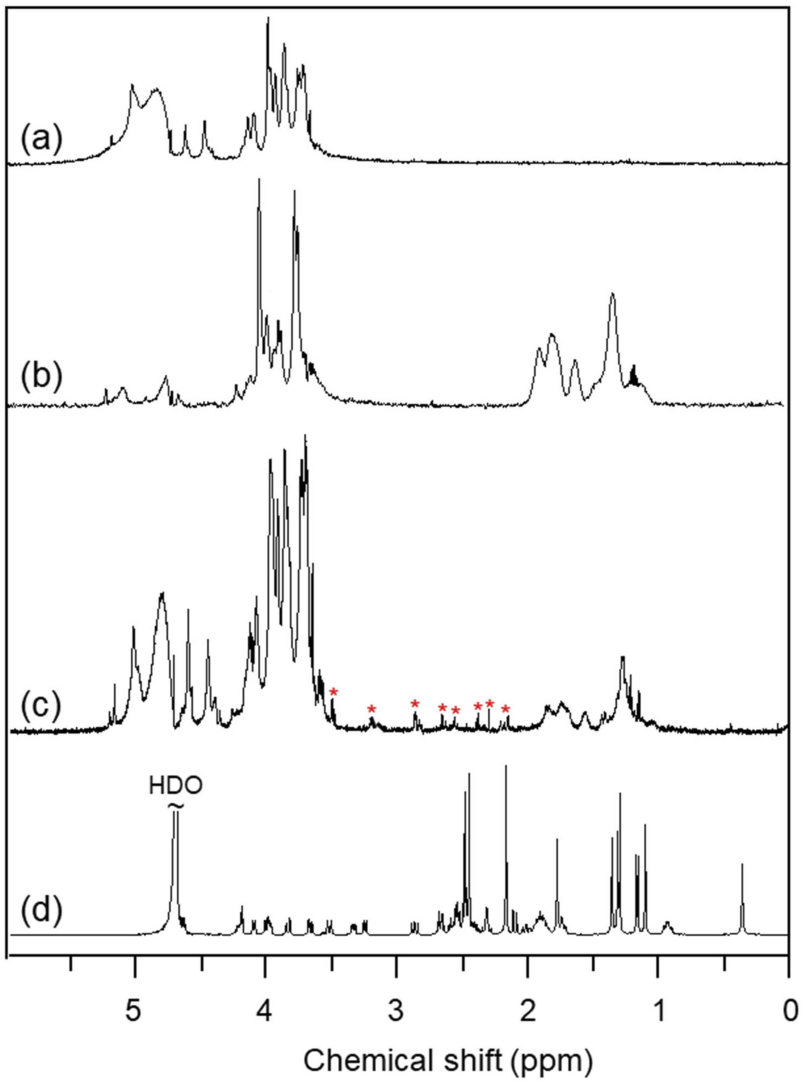

Figure 2 ^{1}H NMR spectra (400 MHz, D_2O, 25°C) of (**A**) sodium alginate, (**B**) the CSAD derivative, (**C**) the CSAD-VB_{12} derivative, and (**D**) vitamin B_{12} (a–c: the signal at δ 4.67 ppm for HDO was suppressed).

Preparation And Physicochemical Property Of CSAD-VB_{12}/Insulin Nanoparticles

To improve the absorption efficacy of insulin by the small intestine after oral administration, insulin-loaded nanoparticles based on the CSAD derivative and the CSAD-VB_{12} derivative were prepared by self-assembly in PBS (pH 7.4). The insulin-loading capacities of the CSAD derivative and the CSAD-VB_{12} derivative were determined to be 32% and 34% using UV–vis spectroscopy.

Figure 4A shows a photo of the CSAD-VB_{12}/insulin solution, in which the Tyndall phenomenon was observed following illumination with a red laser ($\lambda \approx 670$ nm), indicating the formation of nanoparticles in the solution. Morphology of CSAD-VB_{12}/insulin nanoparticles was investigated by scanning electron microscopy (SEM) analysis. They were observed as spherical particles in the sizes ranging from 30 to 50 nm (Figure 4B). The hydrodynamic diameter distribution of CSAD-VB_{12}/insulin nanoparticles was shown in Figure 4C, and their hydrodynamic diameters were determined to be 52.2 ± 3.5 nm. The particle sizes of CSAD-VB_{12}/insulin nanoparticles observed in SEM are smaller than those obtained from ZetaPALS. This is probably because of the different state of CSAD-VB_{12}/insulin nanoparticles, ie, the dried CSAD-VB_{12}/insulin nanoparticles were

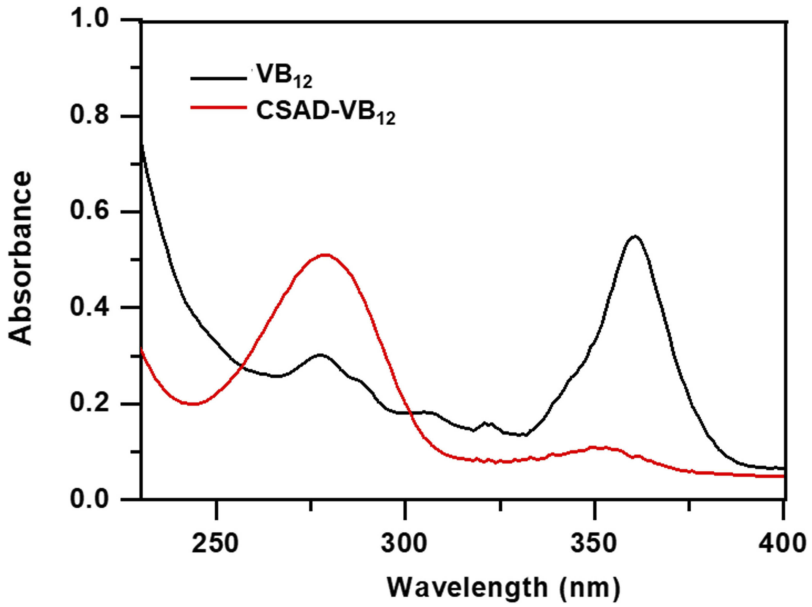

Figure 3 UV-vis spectra of VB_{12} and the CSAD-VB_{12} derivative.

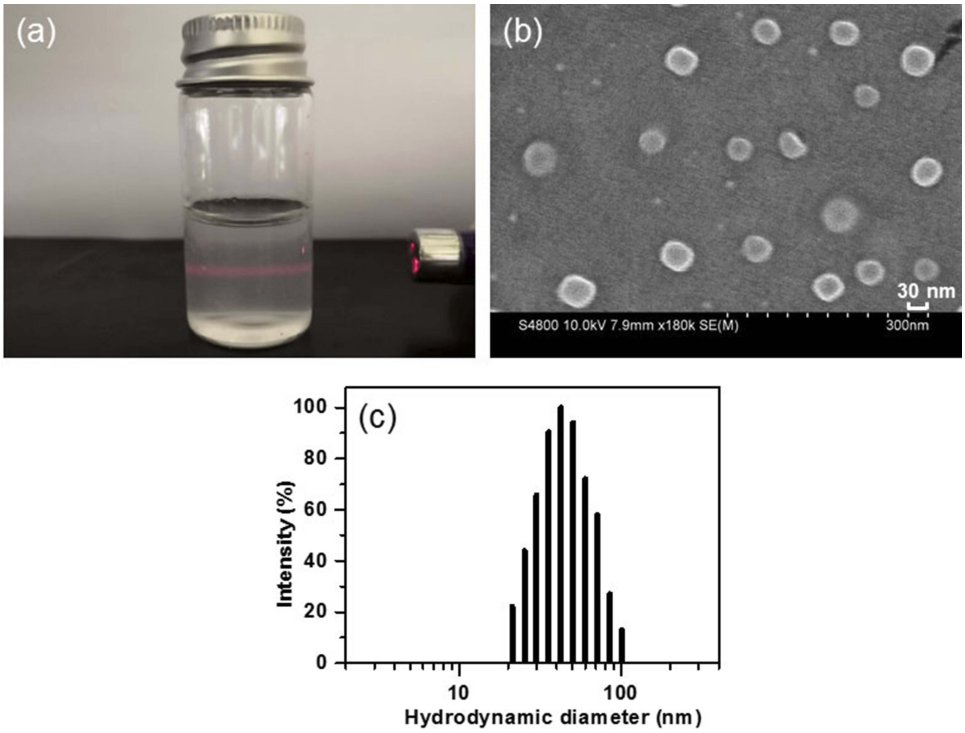

Figure 4 (**A**) Photo of the solution of CSAD-VB_{12}/insulin nanoparticles, (**B**) SEM image of CSAD-VB_{12}/insulin nanoparticles, (**C**) hydrodynamic diameter distribution of CSAD-VB_{12}/insulin nanoparticles.

observed in the SEM image, whereas the hydrated CSAD-VB_{12}/insulin nanoparticles were studied in the ZetaPALS measurement. The zeta potential of CSAD-VB_{12}/insulin nanoparticles is −37.35 ± 0.56 mv.

In Vitro Insulin Release Profiles Of The CSAD-VB_{12}/Insulin Nanoparticles

Figure 5 shows in vitro release profiles of insulin from CSAD/insulin and CSAD-VB_{12}/insulin nanoparticles in

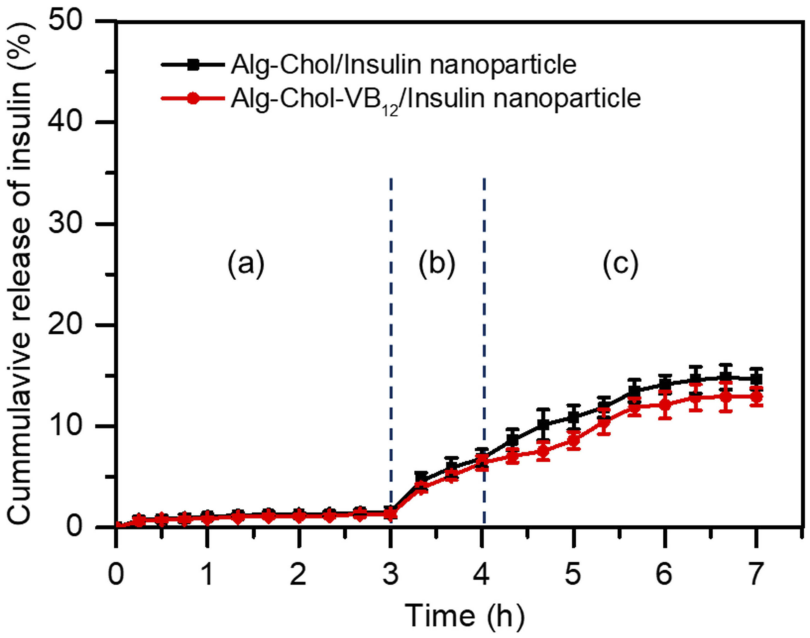

Figure 5 In vitro release profiles of insulin from CSAD-VB_{12}/insulin nanoparticles in the simulated gastrointestinal fluids: (**A**) the simulated stomach fluid, (**B**) the duodenum fluid, and (**C**) the small intestinal fluid.

the simulated gastrointestinal fluids. The cumulative release of insulin from both nanoparticles in the simulated stomach fluid (pH=1.2) was less than 1.5%, suggesting that the CSAD/insulin and CSAD-VB_{12}/insulin nanoparticles could protect insulin in the acidic environment of the stomach. This result was in agreement with that of protein-loaded alginate microcapsules exhibiting negligible protein release (<5%) in the simulated gastric fluid (pH 1.2) [12]. The protection of insulin by the CSAD/insulin and CSAD-VB_{12}/insulin nanoparticles is possibly due to the following reasons. (1) Because the carboxyl groups on the alginate chains lose some of their negative charge, alginate networks tend to shrink at low pH values (pH 1.2) [1]. (2) The hydrophobic interactions between the cholesterol residues of the CSAD-VB_{12} derivative could make the alginate networks denser, which is beneficial in preventing insulin leaking out of nanoparticles. (3) The bulky cholesterol and VB_{12} residues of the CSAD-VB_{12} derivative also contribute in preventing insulin leaking out of nanoparticles.

With increasing the pH value in the simulated duodenum fluid (pH=4.5), the cumulative release of insulin increased to 6.5%. It should be noticed that the cumulative release of insulin from both nanoparticles was still less than 15.0% even in the simulated small intestinal fluid (pH=6.8). These results suggested that a great amount of CSAD/insulin and CSAD-VB_{12}/insulin nanoparticles could safely pass through the stomach and duodenum, and arrive at the small intestine. In comparison, the cumulative release of insulin from the CSAD-VB_{12}/insulin nanoparticles in the simulated intestinal fluids was less than that from the CSAD/insulin nanoparticles. This is probably because the bulky VB_{12} residues of the CSAD-VB_{12} derivative could prevent insulin from leaking out of the CSAD/insulin nanoparticles. With the aid of the CSAD-VB_{12} derivative, the CSAD-VB_{12}/insulin nanoparticles are anticipated to be absorbed by the mucous membrane of small intestine.

Cytotoxicity Analysis

The CSAD and CSAD-VB_{12} derivatives were expected to exert a similar effect of cargo on the intestinal epithelium, which can enable the transport of insulin molecules from the gastrointestinal lumen into the systemic circulation. Therefore, it is necessary to evaluate the toxicities of the CSAD and CSAD-VB_{12} derivatives as well as the CSAD/insulin and CSAD-VB_{12}/insulin nanoparticles to intestinal epithelial cells. The cytotoxicity evaluation was performed using Caco-2 cells as a model to imitate the human intestinal epithelium.[29] The Caco-2 cells retained viability of more than 90% at the concentration of CSAD and CSAD-VB_{12} less than 3 mg/mL for all samples (Figure 6). It should be noticed that the cell viabilities of all samples were still more than 80% even at the high concentration of CSAD and CSAD-VB_{12} (5 and 10 mg/mL). The result proved the non-

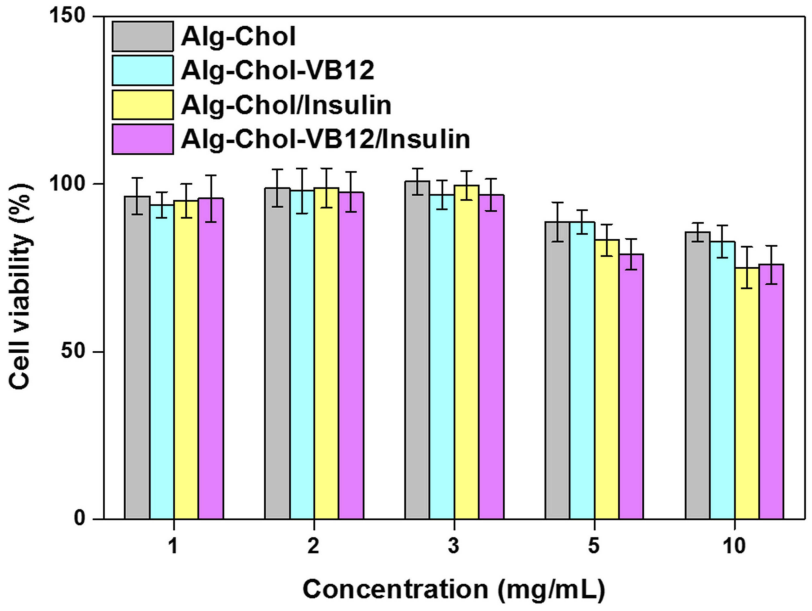

Figure 6 Influence of cell viability of Caco-2 cells incubated with the CSAD and CSAD-VB_{12} derivatives, CSAD/Insulin and CSAD-VB_{12}/Insulin nanoparticles on the concentration of CSAD and CSAD-VB_{12} (n = 3, mean ± standard deviation, P > 0.05).

toxic nature of the CSAD/Insulin and CSAD-VB_{12}/Insulin nanoparticles to Caco-2 cells at the concentration of CSAD and CSAD-VB_{12} less than 3 mg/mL, owing to good biocompatibility of alginate. Therefore, we used these nanoparticles for further studies.

Permeability Of Caco-2 Cell Monolayers For The CSAD-VB_{12}/Insulin Nanoparticles

Previous studies usually used monolayers of Caco-2 cells as a model to evaluate intestinal permeability in vitro.[22,23,30] Studies reported that drugs in vivo human absorption, which were absorbed to >100%, 1–100%, and <1%, had a Papp value >1×10^{-6} cm/s, $1.0\times10^{-7}\sim1.0\times10^{-6}$ cm/s, and <1.0×10^{-7} cm/s, respectively.[30] The permeation properties of the CSAD/Insulin and CSAD-VB_{12}/Insulin nanoparticles through intestinal enterocytes were thus evaluated using the Caco-2 model. As shown in Figure 7A, the Papp values of insulin and the CSAD/Insulin and CSAD-VB_{12}/Insulin nanoparticles increased from $0.3\pm0.02\times10^{-7}$ cm/s, $1.3\pm0.07\times10^{-7}$ cm/s, and $8.4\pm0.3\times10^{-6}$ cm/s at 1 hr to $0.4\pm0.1\times10^{-7}$ cm/s, $1.4\pm0.0868\times10^{-7}$ cm/s, and $10.3\pm0.3\times10^{-6}$ cm/s at 2 hrs, respectively. The lower Papp values of insulin and the CSAD/Insulin nanoparticles suggested their limited transepithelial absorption. It should be noticed that the Papp value of the CSAD-VB_{12}/Insulin nanoparticles is significantly higher than that of insulin and the CSAD/Insulin nanoparticles. This result is consistent with previous studies that the transcellular pathway via the VB_{12} absorption pathway will be one of the best choices for the oral delivery of peptides encapsulated in nanoparticles.[2,31]

A study[32] reported that the drug internalization and the transport efficacy through cell monolayer were substantially improved by VB_{12}-modified nanoparticles. Therefore, we suggested that CSAD-VB_{12}/Insulin nanoparticles could increase the small intestinal absorption efficacy of peptide drugs (insulin) through oral administration.

Endocytosis Of Caco-2 Cell Monolayers For The CSAD-VB_{12}/Insulin Nanoparticles

In order to confirm the endocytosis of Caco-2 cell monolayers for the CSAD-VB_{12}/insulin nanoparticles, confocal laser scanning microscopy was used to record these activities (Figure 7B). In this study, we used insulin-FITC instead of insulin to load with nanoparticles. Therefore, we can observe green fluorescence, when CSAD-VB_{12}/insulin-FITC nanoparticles are endocytosed by Caco-2 cells. Seldom green fluorescence was observed in cytoplasm of Caco-2 cells at the 0 hr, and more and more green fluorescence were accumulated in cellular cytoplasm from 1 hr to 2 hrs (Figure 7B). The intensity of FITC fluorescence was quantified in Figure 7C. These results indicate that CSAD-VB_{12}/insulin-FITC nanoparticles were effectively endocytosed by Caco-2 cells.

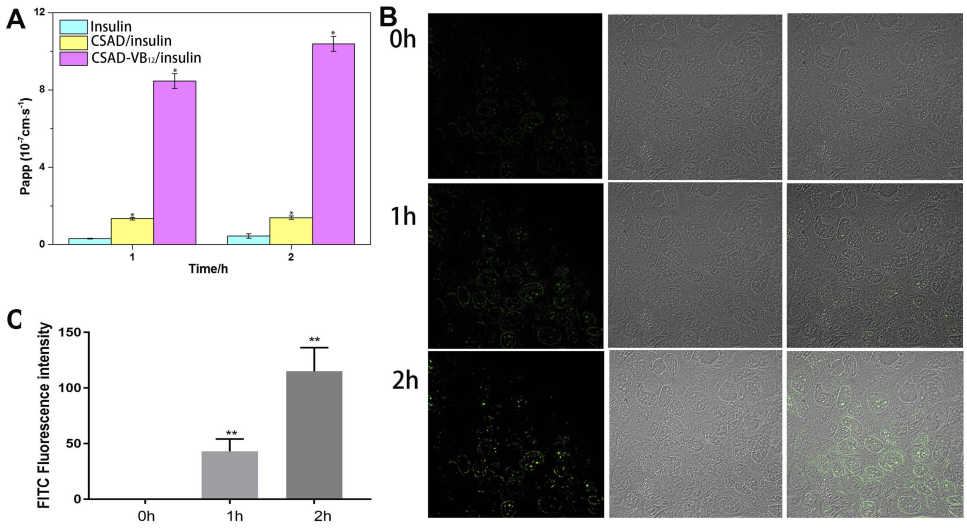

Figure 7 Permeability and cellular uptake study. (**A**) Papp of different insulin formulations: insulin, the CASD/Insulin nanoparticles and the CASD-VB_{12}/Insulin nanoparticles (n = 3; data shown are mean ± SD, *P < 0.05 in comparison with insulin group). (**B**) Confocal laser scanning microscopic images of Caco-2 cells incubated with the CSAD-VB_{12}/FITC-insulin nanoparticles at 37°C for 2 hrs, and their overlay at the 0, 1, and 2 hrs after incubation. (**C**) The quantification of FITC in cells (values represented as the mean ± standard deviation (n = 3), **p <0.01, compared to 0 hr).

GI Retention And Intestinal Absorption For The FITC-Insulin, CSAD/FITC-Insulin Nanoparticles And CSAD-VB_{12}/FITC-Insulin Nanoparticles

In order to evaluate the GI retention effect of test nanoparticles, we firstly used in vivo animal imaging system to obtain the fluorescent signal of FITC-insulin in the GI of T1D mice. As shown in Figure 8A and E, fluorescent signal in GI of both CSAD/FITC-insulin nanoparticles and CSAD-VB_{12}/FITC-insulin nanoparticles could be observed at the 1 hr after oral administration, but that of FITC-insulin had no fluorescent signal, which indicated that in vivo damage of insulin by the proteolytic enzymes in the stomach and intestine can be prevented to control the release of insulin from the formulated nanoparticles. The fluorescent intensity in GI was quantified in Figure 8E. In addition, we observed the isolated small intestine after removing the loosely adherent mucus. The results showed that fluorescent signal of FITC-insulin could be obtained in the group of CSAD/FITC-insulin nanoparticles (Figure 8B2 and F) and CSAD-VB_{12}/FITC-insulin nanoparticles (Figure 8B3 and F), but seldom signal was found in FITC-insulin group (Figure 8B1 and F), which confirmed the results that both CSAD/FITC-insulin and CSAD-VB_{12}/FITC-insulin showed higher intestinal retention effect in intestinal tissue. The fluorescent intensity in isolated small intestine was quantified in Figure 8F.

Secondly, intestinal absorption effect of CSAD/FITC-insulin nanoparticles and CSAD-VB_{12}/FITC-insulin nanoparticles were evaluated by the intestinal loop model of T1D mice. As shown in Figure 8C, there was no green fluorescent signal captured in the intestinal villus cells for FITC-insulin (Figure 8C1 and G), and slight green fluorescent signal was observed in mucus layer for CSAD/FITC-insulin nanoparticles (Figure 8C2 and G). Stronger green fluorescent signals for CSAD-VB_{12}/FITC-insulin nanoparticles were scattered in the villus of the small intestine (Figure 8C3 and G). The fluorescent intensity in intestinal villus cells was quantified in Figure 8G. The preliminary conclusion is that the FITC-insulin-loaded CSAD-VB_{12} nanoparticles were specifically absorbed by the mice small intestine, because VB_{12} can enhance the intestine absorption.

In Vivo Efficacy Of CSAD/FITC-Insulin Nanoparticles And CSAD-VB_{12}/FITC-Insulin Nanoparticles

Type 1 diabetic rats were used to assess efficacy after orally administrating of CSAD/INS (insulin) nanoparticles and CSAD-VB_{12}/INS nanoparticles.

The result showed a sharp drop in blood glucose level within 2 hrs in the group of s.c. injection of free INS, but the oral administration of insulin failed to induce the decrease of blood glucose level. CSAD/INS nanoparticles and CSAD-VB_{12}/INS nanoparticles induced gradual decrease of blood glucose after oral administration. CSAD-VB_{12}/INS nanoparticles induced more obvious reduction of blood glucose level by 54% compared with

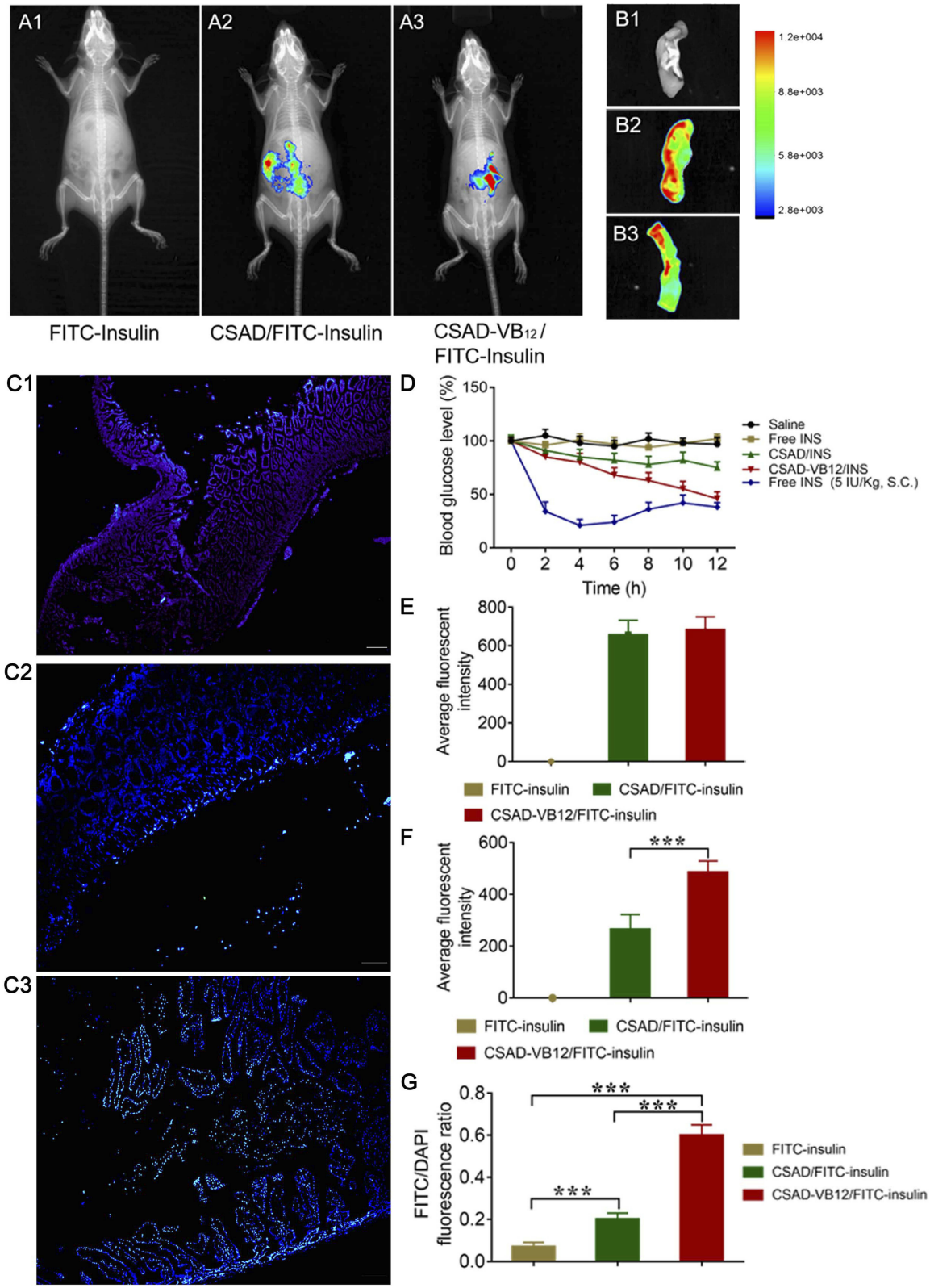

Figure 8 The retention effect and absorption of FITC-insulin, CSAD/FITC-insulin, CSAD-VB_{12}/FITC-insulin in intestine. (**A**) In vivo animal image system showed the fluorescent signal of FITC-insulin (A1) , CSAD/FITC-insulin (A2), CSAD- VB_{12}/FITC-insulin (A3) at the 1 h after oral administration in T1D mice. The fluorescent intensity in GI of each group was quantified in (**E**). (**B**) Representative fluorescence imaging of small intestine from mice treated with FITC-insulin (B1), CSAD/FITC-insulin (B2), CSAD- VB_{12}/FITC-insulin (B3). The fluorescent intensity in isolated small intestine was quantified in (**F**). (**C**) Intestinal absorption of FITC-insulin (C1), CSAD/FITC-insulin (C2), CSAD- VB_{12}/FITC-insulin (C3) after removal of mucus. The fluorescent intension of FITC-insulin in intestinal villus cells was qualified as the rate of FITC/DAPI in (**G**). (**D**) Blood glucose change of T1D mice after oral administration of CSAD/insulin, CSAD- VB_{12}/insulin (insulin, 70 IU/kg, free INS, and saline as control). Subcutaneous (s.c.) injection with insulin at a dose of 5 IU/kg was viewed as a positive control. ***$p < 0.001$ for comparisons with other group.

25% for CSAD/INS group within 12 hrs at the same insulin dose of 70 IU/kg (Figure 8D).

Discussion

Peptide drugs have difficult diffusion across the small intestinal mucus layer and low absorption by epithelium cells, degradation of digestive enzymes (such as pepsin and trypsin) inside the human gastrointestinal tract (GIT), and instabilities in the acidic environment of the stomach, which lead to the low absorption efficacy by oral administration.[33,34]

With the ability of achieving sustained plasma levels of the drug, oral administration is an economical, convenient, and non-invasive method of drug delivery.[32,35] In order to improve the oral delivery efficacy of peptide drug, attempts to use nanotechnology have been promising, and drug release is an important problem in the design of such nanoparticles. Caco-2 cells can form a polarized tight monolayer with microvilli at the apical side after 3 weeks cell cultures.[36] US FDA has recommended researchers used Caco-2 cells to mimic human intestinal metabolism and studied the intestinal absorption of organic compounds.[37,38] Recently, many studies have demonstrated that polymeric nanoparticles possessed the characteristics of longevity, biocompatibility, high stability to solubilize poorly soluble pharmaceutical agents and improve them across physiological barriers in vitro and in vivo.[39,40] For example, a creative polymeric carrier was synthesized by chitosan-functionalized Pluronic P123/F68 micelles to load myricetin (MYR-MCs), which could suppress the proliferation and growth of glioblastoma cells and at the same time induce apoptosis of glioblastoma cells. Notably, MYR-MCs had a high cellular uptake in Caco-2 cells. As stated above, the utilization of polymeric nanoparticles can improve the oral delivery efficacy of classical medicines by passing through intestinal barriers and thus enhance bioavailability through possible transcellular and paracellular pathways.

In addition to the above, the transcellular pathway via the vitamin B12 (VB_{12}) absorption pathway will be one of the best choices for the oral delivery of peptides encapsulated in nanoparticles.[2,31] Koutsouki et al[41] showed that polymeric micelles with linkage to VB_{12} significantly enhanced oral absorption and delivery efficiency and that the process was initiated by the complexation of VB_{12} with IF. Ke et al[42] reported that the drug internalization and the transport efficacy through cell monolayer were substantially improved by VB_{12}-modified nanoparticles. Therefore, we went on to synthesize a CSAD-VB_{12} by the N,N'-dicyclohexylcarbodiimide active method to increase the small intestinal absorption efficacy of peptide drugs through oral administration. In order to measure the effects of CSAD-VB_{12}, insulin was considered as a model peptide drug and the insulin-loaded CSAD-VB_{12} (CSAD-VB_{12}/insulin) nanoparticles with negative zeta potentials were sys in PBS (pH=7.4, Scheme 1B). They finally formed spherical nanoparticles in the size of 30–50 nm using scanning electron microscopy.

Alginate is a linear anionic polysaccharide based on 1,4-β-D-mannuronic acid and α-L-guluronic acid (G) residues.[7] With the advantages of excellent cytocompatibility, biodegradability, chelating ability, non-toxicity, and non-immunogenicity, sodium alginate has been identified as a natural polysaccharide increasing biomedical applications and an effective inhibitor of P-glycoprotein efflux pump limiting oral bioavailability through the transcellular pathway.[8,9] Alginate nanoparticles and microparticles were crosslinked by calcium ions to protect peptide and protein drugs from the electrostatic attraction in low gastric pH value and enzymatic hydrolysis.[12,13] Additionally, alginate nanoparticles and microparticles were commonly coated with chitosan shell so as to enhance their stabilities and absorption efficacies in the small intestine.[12–14] Amphiphilic polysaccharide derivatives, which could assemble to form nanoparticles through intermolecular interactions, are potential drug carriers of peptides (or proteins).[15] Based on our previous work, the amphiphilic sodium alginate derivatives (CSAD) were synthesized to prepare the nanoparticles for improving oral delivery efficacy of peptide drugs.[7] Our experiment to measure Papp showed that the lower Papp values of insulin and the CSAD/Insulin nanoparticles indicated their limited transepithelial absorption. Importantly, the Papp value of the CSAD-VB_{12}/Insulin nanoparticles was significantly higher than that of insulin and the CSAD/Insulin nanoparticles. The result thus evidences that the VB_{12} pathway is effective in the transport of insulin-loaded CSAD-VB_{12} nanoparticles through model intestinal cell monolayers, resulting in the enhancement of the amount of insulin transported. We also used T1D mice model to confirm CSAD-VB_{12}/Insulin nanoparticles exhibited great GI retention effect, intestinal absorption, and in vivo efficacy.

According to these findings, the CSAD-VB_{12}/Insulin nanoparticles were used to enhance the small intestinal absorption efficacy of insulin. They were nontoxic for small intestinal and exerted high permeation by intestinal enterocytes. Therefore, the CSAD-VB_{12} demonstrates significant and efficient potential for oral delivery of peptide drugs.

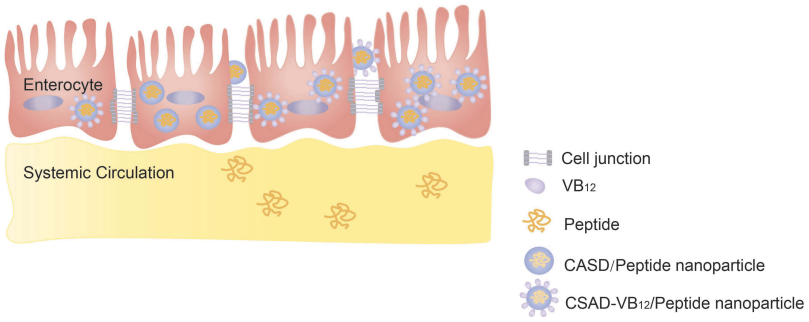

Scheme 3 Proposed schematic presentation of CASD-VB_{12}/Insulin nanoparticles permeating through monolayer of intestinal enterocytes.

Conclusion

Our study showed that small intestinal absorption efficacy of the CSAD-VB_{12}/Insulin nanoparticles was significantly higher than that of peptide and the CSAD/Insulin nanoparticles. The result thus evidences that the VB_{12} pathway is effective in the transport of insulin-loaded CSAD-VB12 nanoparticles through in vitro and in vivo model, resulting in the enhancement of the amount of insulin transported. Importantly, they were nontoxic for small intestinal and exerted high permeation by intestinal enterocytes. Therefore, the CSAD-VB_{12} demonstrates significant and efficient potential for oral delivery of peptide drugs (Scheme 3).

Abbreviations

GI, the human gastrointestinal tract; VB_{12}, vitamin B_{12}; CSAD, amphiphilic sodium alginate derivatives; CSAD-VB_{12}, amphiphilic sodium alginate derivatives containing vitamin $B_{12;}$ CDI, N,N'-carbonyldiimidazole; DCC, N,N'-dicyclohexylcarbodiimide; DMAP, 4-(N,N'-dimethylamino) pyridine; DMSO, dimethyl sulfoxide; DS, degree of substitution; Papp, apparent permeability. INS, insulin; AFI, the average fluorescent intensity.

Acknowledgments

This work was supported by National Natural Science Foundation of China (81571105), the Science and Technology Planning Project of Guangzhou, Guangdong Province, China (201607010249), the Special Funds for Public Welfare Research and Capacity Building of Guangdong Province in China (2016A020222017), the Key Project of Guangdong Natural Science Foundation of China (2017B030311007), and the National Natural Science Foundation of China (30900650, 81372501, 81572260 and 81773299). We thank Ms. Krsna Moody Muscheck for editing and revising the manuscript.

Disclosure

The authors report no conflicts of interest in this work.

References

1. McClements DJ. Encapsulation, protection, and delivery of bioactive proteins and peptides using nanoparticle and microparticle systems: a review. *Adv Colloid Interface Sci*. 2018;253:1–22. doi:10.1016/j.cis.2018.02.002
2. Lundquist P, Artursson P. Oral absorption of peptides and nanoparticles across the human intestine: opportunities, limitations and studies in human tissues. *Adv Drug Deliver Rev*. 2016;106:256–276. doi:10.1016/j.addr.2016.07.007
3. Yun Y, Cho YW, Park K. Nanoparticles for oral delivery: targeted nanoparticles with peptidic ligands for oral protein delivery. *Adv Drug Deliver Rev*. 2013;65(6):822–832. doi:10.1016/j.addr.2012.10.007
4. Lai MH, Wang JN, Tan JY, et al. Preparation, complexation mechanism and properties of nano-complexes of Astragalus polysaccharide and amphiphilic chitosan derivatives. *Carbohyd Polym*. 2017;161:261–269. doi:10.1016/j.carbpol.2016.12.068
5. Wang JN, Tan JY, Luo JH, et al. Enhancement of scutellarin oral delivery efficacy by vitamin B12-modified amphiphilic chitosan derivatives to treat type II diabetes-induced retinopathy. *J Nanobiotechnol*. 2017;15. doi:10.1186/s12951-017-0251-z
6. Czuba E, Diop M, Mura C, et al. Oral insulin delivery, the challenge to increase insulin bioavailability: influence of surface charge in nanoparticle system. *Int J Pharm*. 2018;542(1–2):47–55. doi:10.1016/j.ijpharm.2018.02.045
7. Yang LQ, Zhang BF, Wen LQ, Liang QY, Zhang LM. Amphiphilic cholesteryl grafted sodium alginate derivative: synthesis and self-assembly in aqueous solution. *Carbohyd Polym*. 2007;68(2):218–225. doi:10.1016/j.carbpol.2006.12.020
8. Yu Z, Li HJ, Zhang LM, Zhu ZH, Yang LQ. Enhancement of phototoxicity against human pancreatic cancer cells with photosensitizer-encapsulated amphiphilic sodium alginate derivative nanoparticles. *Int J Pharm*. 2014;473(1–2):501–509. doi:10.1016/j.ijpharm.2014.07.046
9. Malhaire H, Gimel JC, Roger E, Benoit JP, Lagarce F. How to design the surface of peptide-loaded nanoparticles for efficient oral bioavailability? *Adv Drug Deliver Rev*. 2016;106:320–336. doi:10.1016/j.addr.2016.03.011
10. Goswami S, Bajpai J, Bajpai A. Calcium alginate nanocarriers as possible vehicles for oral delivery of insulin. *J Exp Nanosci*. 2014;9(4):337–356. doi:10.1080/17458080.2012.661472
11. Zhang ZP, Zhang RJ, Zou LQ, McClements DJ. Protein encapsulation in alginate hydrogel beads: effect of pH on microgel stability, protein retention and protein release. *Food Hydrocolloid*. 2016;58:308–315. doi:10.1016/j.foodhyd.2016.03.015

12. Ghaffarian R, Perez-Herrero E, Oh H, Raghavan SR, Muro S. Chitosan-alginate microcapsules provide gastric protection and intestinal release of ICAM-1-targeting nanocarriers, enabling GI targeting in vivo. *Adv Funct Mater*. 2016;26(20):3382–3393. doi:10.1002/adfm.201600084
13. Zhang YL, Wei W, Lv PP, Wang LY, Ma GH. Preparation and evaluation of alginate-chitosan microspheres for oral delivery of insulin. *Eur J Pharm Biopharm*. 2011;77(1):11–19. doi:10.1016/j.ejpb.2010.09.016
14. Bagre AP, Jain K, Jain NK. Alginate coated chitosan core shell nanoparticles for oral delivery of enoxaparin: in vitro and in vivo assessment. *Int J Pharmaceut*. 2013;456(1):31–40. doi:10.1016/j.ijpharm.2013.08.037
15. Ayame H, Morimoto N, Akiyoshi K. Self-assembled cationic nanogels for intracellular protein delivery. *Bioconjugate Chem*. 2008;19(4):882–890. doi:10.1021/bc700422s
16. Nagahama K, Mori Y, Ohya Y, Ouchi T. Biodegradable nanogel formation of polylactide-grafted dextran copolymer in dilute aqueous solution and enhancement of its stability by stereocomplexation. *Biomacromolecules*. 2007;8(7):2135–2141. doi:10.1021/bm070206t
17. Heinze T, Liebert T, Koschella A. *Esterification of Polysaccharides*. New York: Springer Berlin Heidelberg; 2006:88–89.
18. Russell-Jones GJ, Westwood SW, Farnworth PG, Findlay JK, Burger HG. Synthesis of LHRH antagonists suitable for oral administration via the vitamin B12 uptake system. *Bioconjugate Chem*. 1995;6(1):34–42.
19. Russell-Jones GJ, Westwood SW, Habberfield AD. Vitamin B12 mediated oral delivery systems for granulocyte-colony stimulating factor and erythropoietin. *Bioconjugate Chem*. 1995;6(4):459–465.
20. Okuda K. Discovery of vitamin B12 in the liver and its absorption factor in the stomach: a historical review. *J Gastroenterol Hepatol*. 1999;14(4):301–308.
21. Petrus AK, Fairchild TJ, Doyle RP. Traveling the vitamin B12 pathway: oral delivery of protein and peptide drugs. *Angew Chem Int Ed Engl*. 2009;48(6):1022–1028. doi:10.1002/anie.200800865
22. Borkar N, Chen ZZ, Saaby L, et al. Apomorphine and its esters: differences in Caco-2 cell permeability and chylomicron affinity. *Int J Pharm*. 2016;509(1–2):499–506. doi:10.1016/j.ijpharm.2016.06.010
23. Sevin E, Dehouck L, Fabulas-da Costa A, et al. Accelerated Caco-2 cell permeability model for drug discovery. *J Pharmacol Tox Met*. 2013;68(3):334–339. doi:10.1016/j.vascn.2013.07.004
24. *Chinese Pharmacopoeia*. Beijing: China Medicine Science Press; 2015:72.
25. Sun LZ, Wang YZ, Jiang TY, et al. Novel chitosan-functionalized spherical nanosilica matrix as an oral sustained drug delivery system for poorly water-soluble drug carvedilol. *Acs Appl Mater Inter*. 2013;5(1):103–113. doi:10.1021/am302246s
26. Reti-Nagy K, Malanga M, Fenyvesi E, et al. Endocytosis of fluorescent cyclodextrins by intestinal Caco-2 cells and its role in paclitaxel drug delivery. *Int J Pharm*. 2015;496(2):509–517. doi:10.1016/j.ijpharm.2015.10.049
27. Tian H, He Z, Sun C, et al. Uniform core-shell nanoparticles with thiolated hyaluronic acid coating to enhance oral delivery of insulin. *Adv Healthc Mater*. 2018;7(17):e1800285. doi:10.1002/adhm.201800285
28. Francis MF, Cristea M, Winnik FM. Exploiting the vitamin B-12 pathway to enhance oral drug delivery via polymeric micelles. *Biomacromolecules*. 2005;6(5):2462–2467. doi:10.1021/bm0503165
29. Neves AR, Queiroz JF, Costa Lima SA, Figueiredo F, Fernandes R, Reis S. Cellular uptake and transcytosis of lipid-based nanoparticles across the intestinal barrier: relevance for oral drug delivery. *J Colloid Interface Sci*. 2016;463:258–265. doi:10.1016/j.jcis.2015.10.057
30. Artursson P, Karlsson J. Correlation between oral drug absorption in humans and apparent drug permeability coefficients in human intestinal epithelial (Caco-2) cells. *Biochem Biophys Res Commun*. 1991;175(3):880–885. doi:10.1016/0006-291x(91)91647-u
31. Wang J, Tan J, Luo J, et al. Enhancement of scutellarin oral delivery efficacy by vitamin B12-modified amphiphilic chitosan derivatives to treat type II diabetes induced-retinopathy. *J Nanobiotechnology*. 2017;15(1):18. doi:10.1186/s12951-017-0305-2
32. Frutos G, Prior-Cabanillas A, Paris R, Quijada-Garrido I. A novel controlled drug delivery system based on pH-responsive hydrogels included in soft gelatin capsules. *Acta Biomater*. 2010;6(12):4650–4656. doi:10.1016/j.actbio.2010.07.018
33. Jabir MS, Taha AA, Sahib UI, Taqi ZJ, Al-Shammari AM, Salman AS. Novel of nano delivery system for Linalool loaded on gold nanoparticles conjugated with CALNN peptide for application in drug uptake and induction of cell death on breast cancer cell line. *Mat Sci Eng C-Mater*. 2019;94:949–964. doi:10.1016/j.msec.2018.10.014
34. Wu C, Hu W, Wei QC, et al. Controllable growth of core-shell nanogels via esterase-induced self-assembly of peptides for drug delivery. *J Biomed Nanotechnol*. 2018;14(2):354–361. doi:10.1166/jbn.2018.2492
35. Wei W, Ma GH, Wang LY, Wu J, Su ZG. Hollow quaternized chitosan microspheres increase the therapeutic effect of orally administered insulin. *Acta Biomater*. 2010;6(1):205–209. doi:10.1016/j.actbio.2009.06.005
36. Naruhashi K, Kurahashi Y, Fujita Y, et al. Comparison of the expression and function of ATP binding cassette transporters in Caco-2 and T84 cells on stimulation by selected endogenous compounds and xenobiotics. *Drug Metab Pharmacol*. 2011;26(2):145–153. doi:10.2133/dmpk.DMPK-10-RG-075
37. Dempe JS, Scheerle RK, Pfeiffer E, Metzler M. Metabolism and permeability of curcumin in cultured Caco-2 cells. *Mol Nutr Food Res*. 2013;57(9):1543–1549. doi:10.1002/mnfr.201200113
38. Yu SH, Tang DW, Hsieh HY, et al. Nanoparticle-induced tight-junction opening for the transport of an anti-angiogenic sulfated polysaccharide across Caco-2 cell monolayers. *Acta Biomater*. 2013;9(7):7449–7459. doi:10.1016/j.actbio.2013.04.009
39. Wang G, Wang JJ, Tang XJ, Du L, Li F. In vitro and in vivo evaluation of functionalized chitosan-Pluronic micelles loaded with myricetin on glioblastoma cancer. *Nanomed-Nanotechnol*. 2016;12(5):1263–1278. doi:10.1016/j.nano.2016.02.004
40. Jaruszewski KM, Ramakrishnan S, Poduslo JF, Kandimalla KK. Chitosan enhances the stability and targeting of immuno-nanovehicles to cerebrovascular deposits of Alzheimer's disease amyloid protein. *Nanomed-Nanotechnol*. 2012;8(2):250–260. doi:10.1016/j.nano.2011.06.008
41. Koutsouki E. Exploiting the vitamin B12 uptake pathway to help fight obesity. *Future Med Chem*. 2013;5(17):2016.
42. Ke ZY, Guo H, Zhu X, Jin Y, Huang Y. Efficient peroral delivery of insulin via vitamin B-12 modified trimethyl chitosan nanoparticles. *J Pharm Pharm Sci*. 2015;18(2):155–170.